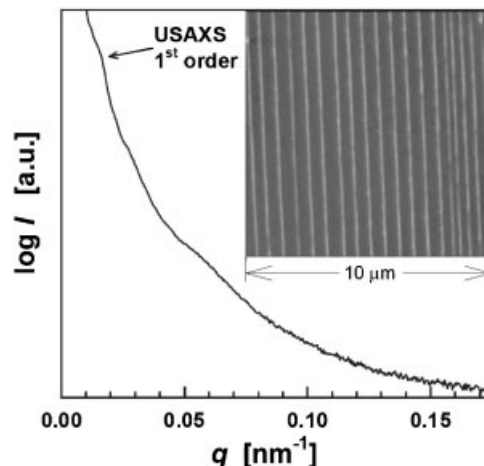


Ultra-Small-Angle X-Ray Scattering Study of PET/PC Nanolayers and Comparison to AFM Results

Fernando Ania,* Inés Puente-Orench, Francisco J. Baltá Calleja, Devang Khariwala, Anne Hiltner, Eric Baer, Stephan V. Roth

The forced assembly of two immiscible polymers, produced by layer-multiplying co-extrusion, is analyzed by means of USAXS. Comparison of scattering and AFM results sheds light on many details of the nanolayered structure in PET/PC films. The role played by the volume concentration and cold crystallization of PET on the experimental scattering is discussed. The appearance of at least two scattering maxima in all cases, corresponding to higher orders of the same repeating distance, accounts for the high regularity of the developed nanostructure. It is finally shown that long spacing values, derived from a localized area in AFM, are in a good agreement with the USAXS values averaged over much larger areas.



Introduction

Microlayering is an attractive approach to design polymer architectures for specific purposes. New technologies often require the production of ultra-thin polymer layers which may affect the physical properties of the highly constrained polymer chains. It is well known that physical properties like the glass transition temperature, toughness, crystallinity, and molecular orientation may undergo significant changes as thickness decreases below the nanometer scale.^[1–6] At this level, even the thinnest interphase may become of the utmost importance as it could be considered a new phase by itself. Layer-multiplying co-extrusion of two different polymers has been shown to produce rather uniform assemblies with up to thousands of layers. Assemblies with layers thinner

F. Ania, I. Puente-Orench, F. J. Baltá Calleja
Instituto de Estructura de la Materia, CSIC, Serrano 119, E-28006
Madrid, Spain

Fax: +34 91 564 2431; E-mail: emfernando@iem.cfmac.csic.es

I. Puente-Orench

Current address: Instituto de Ciencia de Materiales de Aragón,
CSIC – Institut Laue Langevin 6, rue Jules Horowitz, BP 156-38042
Grenoble Cedex 9, France

D. Khariwala, A. Hiltner, E. Baer

Department of Macromolecular Science, Case Western Reserve
University, 2100 Adelbert Road, Cleveland, Ohio 44106-7202, USA
S. V. Roth

Deutsches Elektronen Synchrotron (HASYLAB), Notkestr. 85,
D-22603 Hamburg, Germany

than 10 nm have been recently obtained by this method.^[7] It is known that such structures can be resolved in AFM images and local average layer thicknesses have been measured.^[8] However, if statistically significant information on larger scale areas is required, scattering methods have to be used. Among them, grazing incidence small angle X-ray scattering (GISAXS) is a powerful technique that provides information on the surface structure of polymer thin films.^[9] This technique requires perfectly flat samples with a very small surface roughness. As the investigated samples do not fulfill such requirements, a transmission technique such as ultra-small-angle X-ray scattering (USAXS) was applied. USAXS experiments have been successfully carried out for the last 15 years in connection with the development of specific synchrotron radiation beam-lines. These investigations have been mainly focused on colloidal dispersions, nanoporous materials, complex fluids, nanocomposites, and polymer systems.^[10–14]

The aim of the present study is to report recent results concerning the analysis of the USAXS arising from the electron density difference of alternating nanolayers of two immiscible polymers, one crystallizable poly(ethylene terephthalate) (PET) and the other one non-crystallizable polycarbonate (PC), and to compare these results with AFM images. Coextruded PET/PC films constitute a new kind of multilayered tape consisting of two macroscopically ductile polymers which shows an interesting transition of the microdeformation mechanism which is dependent on the thickness of the individual layers.^[15] One of the benefits of incorporating PET to the system is its ability to crystallize during annealing. This fact offers the opportunity of investigating the variation of the mechanical behavior of the material as PET crystallization develops.^[16,17] On the other hand, PET/PC nanolayers represent a model system to study polymer crystallization in a confined environment (in between PC layers).^[6]

As a final point, it is worth pointing out that this is the first time that we are capable to detect, using USAXS, well-defined large spacings up to 500 nm from a nanolayered structure with very small density differences ($\approx 0.15 \text{ g} \cdot \text{cm}^{-3}$).

Experimental Part

Sample Preparation

The materials used were a Dow Calibre PC with a measured density $1.1913 \text{ g} \cdot \text{cm}^{-3}$ and an M&G Cleartuff PET with amorphous density $1.3363 \text{ g} \cdot \text{cm}^{-3}$, both having molecular weights of about 30 000 and glass transition temperatures of 150 and 75 °C, respectively. Nanolayered assemblies with 4 096 and 1 024 layers and PET/PC volume ratios of 70:30, 50:50, 30:70, 20:80, and 10:90 prepared by the layer-multiplying co-extrusion

method, were used in this study. As film thicknesses vary in the range of 100–300 nm, the nominal long spacings L_{nom} are in the range of 50–500 nm. The size of the interphase between the PET and the PC layers is not known. In the case of PETG/PC, where PETG is an amorphous polyester, it has been estimated to be 27 nm by means of the oxygen permeability dependence on layer thickness.^[18] For other immiscible polymer pairs measured by the same method, the interphase thickness ranges between 4 and 30 nm. As prepared, and due to the rapid quenching on a chill roll equipped with an air knife at the end of the extrusion process, the PET/PC samples were amorphous. Some of them were later heated at various constant temperatures, between 100 and 165 °C for 30 min, to induce partial crystallization in the PET layers.

Techniques

X-ray scattering experiments were performed at the beam-line BW4 (USAXS) of the DORIS III storage ring at HASYLAB/DESY (Hamburg). The X-ray wavelength λ was fixed to 0.138 nm. The scattered intensity was recorded using a two-dimensional Mar CCD detector, in 2048×2048 pixel arrays. The sample detector distance was 12.9 m which, using a beam size of $400 \times 400 \mu\text{m}^2$, gives spatial resolution limits between 30 and 650 nm.^[19] The polymer films, 2 mm wide, were placed with the upper and lower surfaces parallel to the X-ray beam (Z-axis in the scheme of Figure 1). Due to the fact that the films were thinner than the beam size, both limiting surfaces were always illuminated at a grazing incidence angle, giving rise to a very strong meridional scattering which completely masked the USAXS information from the nanolayered structure (Figure 1, left image). By changing the incident angle to $\alpha = 5^\circ$, the grazing incidence scattering could be avoided at the only cost of a slight distortion of the two-dimensional pattern (Figure 1, central image). With this layout, typical USAXS patterns show a meridional scattering yielding information on the nanolayered structure (the measured long spacings, because of the incident angle, should be increased by less than half percent to get the real values) and an additional off-equatorial scattering. Such scattering streak apparently depends on the incident angle α ,^[20] but becomes truly equatorial and independent of α (Figure 1, right image) by rotating the sample by a certain small angle ω until the extrusion direction becomes parallel to the X-ray beam. These observations are consistent with the presence of certain electron density inhomogeneities along the extrusion direction which have been generally identified as aligned microvoids.^[21]

Meridional scans of the two-dimensional patterns were obtained by projecting the intensity into the meridian. Such scans show the same details as the one-pixel meridional cuts but with improved statistics. Background subtraction and correction due to primary beam intensity were applied.

Atomic force microscopy (AFM) imaging was performed using the tapping mode of a Nanoscope IIIa (Digital Instruments). Phase and height images were recorded simultaneously. Specimens were cut from the center of the extruded films and imaging was done in the central portion of the specimen cross-section, which was sectioned perpendicular to the plane of the film with an ultramicrotome (MT6000-XL from RMC, Tucson, AZ, USA). For this purpose, a film specimen was embedded in 5 min epoxy and cured

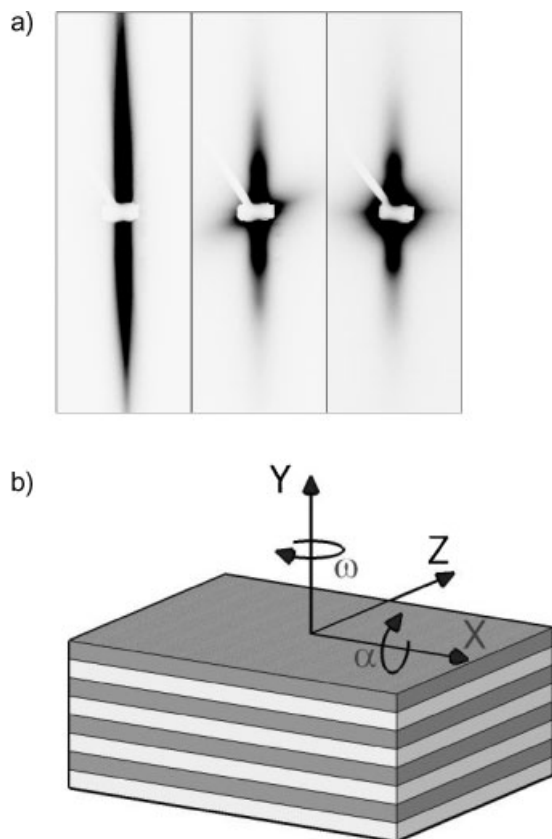


Figure 1. USAXS patterns corresponding to an initial film position with incident beam at $\alpha = 0^\circ$ (left), 5° (center), and after rotation by $\omega \approx 3^\circ$ (right). Rotations of the sample are sketched in the lower part of the figure in relation to the X-ray beam which is parallel to the Z-axis.

overnight at 23°C . Cured specimens were microtomed at 23°C at a cutting speed of $0.5\text{ mm} \cdot \text{s}^{-1}$. The long spacings, consisting of a pair of PET and PC layers, were measured from the AFM phase images which most clearly revealed the layered film structure. The statistical distribution of the long spacings was then compiled. In the case of the sample of PET/PC (70:30) with 1024 layers about 100 pairs of layers were measured and in the case of the 30:70 sample with 4096 layers about 50 pairs of layers were considered.

Results and Discussion

USAXS Experiments

Figure 2 shows the USAXS meridional scans for three different PET/PC nanolayered films, with nominal repeating distances for pairs of alternating layers of 470, 165, and 85 nm, respectively. The nominal distances were simply calculated by dividing the film thickness by half the number of layers. These samples were previously annealed at 150°C for 30 min to induce a certain degree of crystallinity inside the PET layers which increases the density contrast in relation to the PC layers. The scattered

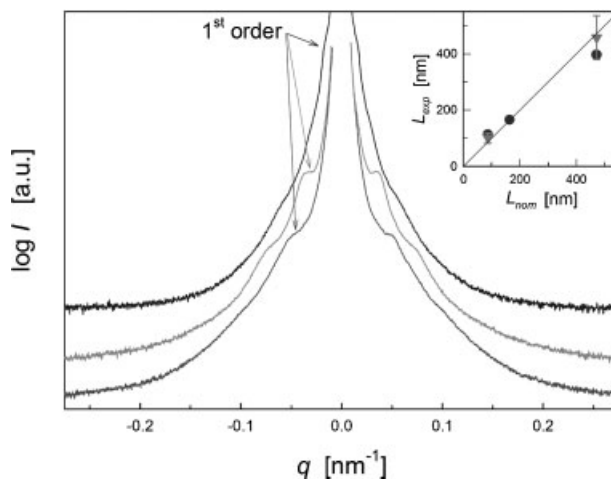


Figure 2. USAXS profiles along the meridian versus scattering vector q for three different multilayered systems having nominal repeating distances L_{nom} (from top to bottom) of 470, 165, and 85 nm. The curves have been shifted along the intensity axis for clarity. Inset: Measured USAXS (circles) and AFM (triangles) long spacings as a function of nominal values.

intensity in logarithmic scale is represented as a function of the scattering vector q (where $q = 2\pi s$ and $s = 2\sin\theta/\lambda$). It is noteworthy that, for all the samples, more than one scattering peak, corresponding at least to two different orders of the same repeating unit, can be observed. The USAXS maxima, after corrections and empty scattering subtraction, were fitted to Lorentz functions and their amplitude and angular position were analyzed. At this point, we are aware that more advanced methods for the structural assessment make use of the correlation function.^[22] However valuable preliminary information can also be obtained from the study of the long spacings, which can be immediately derived from the angular position of the first USAXS maxima by simply using Bragg's law. The long period represents the average distance between regions of equivalent electronic density (i.e., in our multilayer materials, the average distance between PET layers or PC layers).

AFM Imaging

Figure 3a and b, respectively, illustrate height (left) and phase images (right) of the central portion of the cross-section of samples with $L_{\text{nom}} = 470$ and 85 nm. All images show well-defined PET and PC layers with sharp interfaces. Comparison of two different areas along the extruded films indicates that the long spacings are essentially the same and the volume ratio between PET and PC only shows little variation which is somewhat larger in the 70:30 composition.

The statistical distribution of the long spacings from Figure 3a and b is shown in Figure 4a and b, respectively.

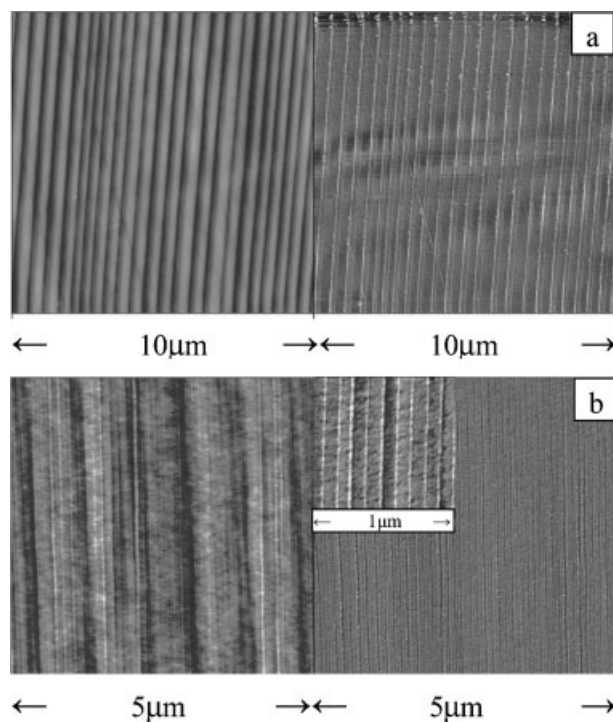


Figure 3. Height (left) and phase (right) AFM images of (a) 70:30 sample with 1024 layers ($L_{\text{nom}} = 470$ nm) and (b) PET/PC (30:70) sample with 4096 layers ($L_{\text{nom}} = 85$ nm). The insert in (b) shows the layers at higher resolution.

At first sight, in both cases, the average long spacing (457 ± 78 and 100 ± 18 nm) measured from AFM correlates well with the nominal long spacings (470 and 85 nm).

The inset in Figure 2 depicts the experimental long spacings, derived from the use of Bragg's law and AFM measurements, as a function of the nominal repeating distances. The error bars of the former are approximately represented by the vertical size of the symbols used. The continuous line in the plot represents the locus of points where experimental and nominal values coincide. Not only a fair relationship between USAXS and AFM values but also between all the experimental values and the nominal ones can be observed. However, a closer look to the results reveals that the thinner experimental long spacings are slightly larger than the corresponding nominal value, while the opposite behavior occurs for the repeating distance corresponding to the thickest layers. The differences are much clearer for the USAXS data. This result could account for a possible tendency of thinnest layers to breakup and not contribute to the scattering, yielding an average long spacing larger than the one expected. It has been previously reported that thin layers of high density poly(ethylene) (PE) coextruded between layers of polystyrene (PS) also show considerable layer breakup.^[23] In the case of the thickest layers, it will be shown below that the samples may be composed of regions with shorter interlayer distances.

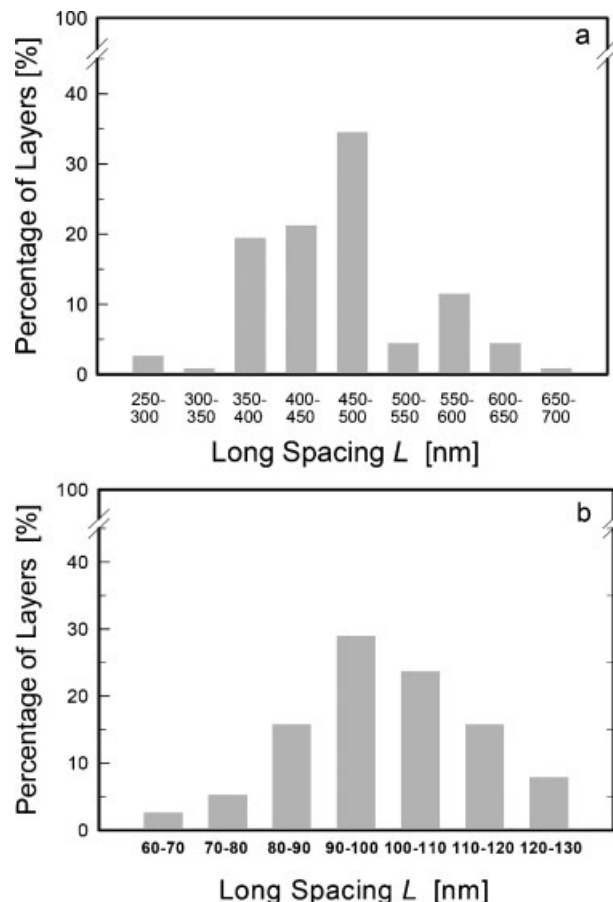


Figure 4. Statistical distribution of the long spacings derived from same samples as in Figure 3: (a) sample with 1024 layers and (b) 4096 layers.

Annealing Behavior

The next question arises as to what is the influence of annealing temperature on the packing of the nanolayered structure. Figure 5 illustrates the USAXS patterns of the PET/PC (70:30) nanolayered sample with an initial long period of 175 nm (similar results can be found for the samples with initial long periods of 470 and 85 nm). One observes a clear scattering intensity increase when the samples are heated for 30 min at different increasing temperatures that are above the glass transition temperature of PET ($T_g = 75$ °C). It also means that the total scattering power increases. Taking into account that the sample volume remains constant and admitting a two-phase model, the scattering power is proportional to the invariant Q which is defined as^[22]

$$Q \sim (\rho_2 - \rho_1)^2 v(1 - v) \quad (1)$$

The second term in Equation (1), $v(1 - v)$, is related to the volume fraction of the two components in the PET/PC

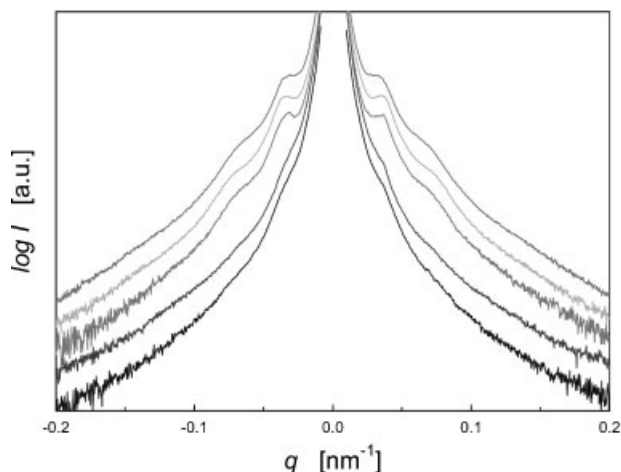


Figure 5. Influence of annealing temperature T_a on the USAXS meridional profiles of a 70:30 PET/PC nanolayered sample with $L_{\text{nom}} = 165$ nm. From top to bottom: $T_a = 165, 150, 132, 100$ °C, and without heat treatment. Curves are shifted along the intensity axis for clarity.

system, which, in our case, remains constant. Therefore, the intensity increase must be due to a larger electron density difference ($\rho_2 - \rho_1$) between the alternating layers of PET and PC. Considering the annealing temperatures used, which are not expected to provoke drastic changes in PC while they certainly induce a certain degree of crystallization in the PET layers, the higher electron density contrast can be ascribed to a densification effect on the PET nanolayers. It must be emphasized that PET crystallites growing inside the PET layers are much smaller than the angular range covered by USAXS and they only contribute, once a certain degree of crystallization is reached, to the growth of the average electron density of the PET layers as a whole.^[6]

On the other hand, for the three studied materials and all annealing temperatures, the angular position of the observed USAXS peaks only shows minor changes. Figure 6

collects the calculated long spacings and most of them can be considered to be constant within experimental error (relative error is around 5%). Some of the larger deviations can be explained by changes in the extruded film thickness. This means that, on annealing, the nanolayered architecture is well preserved even at temperatures which are slightly higher than the glass temperature of both constituent polymers, PET, and PC [T_g (PC) ≈ 150 °C].

Most interesting is the fact that, for all samples (with only one exception), at least two scattering peaks are observed. The number of scattering peaks even increases for the samples with the longest nominal interlayer spacing. It is known that the Porod region, in which any oscillations of the scattering curve of an ideal two-phase system are faded away, generally starts after the second order of the long period peak.^[23] It is then difficult to consider that three or more peaks can be increasing orders of the same periodicity. In fact, taking into account the values of the angular position of the USAXS maxima, it must be concluded that the shortest spacing of the material with $L_{\text{nom}} = 470$ nm is probably related to a different repeating distance. Thus, the 30:70 PET/PC system seems to be predominantly composed of regions with an average long spacing similar to the nominal value and of a smaller proportion of other regions which show a much shorter average layer thickness. Taking into account that AFM results only correspond to central areas of the cross-section whereas the X-ray beam illuminates the whole sample and that a bimodal distribution in the layer thicknesses has never been found by AFM, it could be tentatively concluded that those regions with a shorter layer thickness could well be located close to the film surfaces. Due to the extrusion process, it is evident that close to the film surfaces (friction with the walls) more irregularities of the nanostructure are to be expected. The use of a future microfocus USAXS beam-line, as the one planned for the third generation PETRA III synchrotron source at DESY (Hamburg), could help to solve this question.

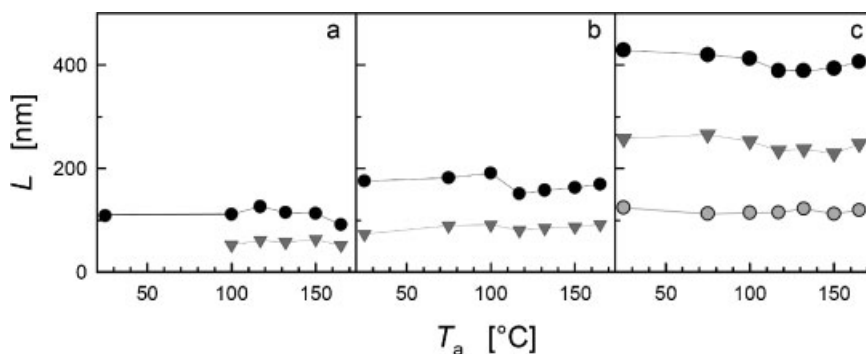


Figure 6. USAXS spacings, as a function of annealing temperature T_a , calculated from the different peaks found in PET/PC samples with nominal repeating distance L_{nom} of: (a) 85 nm (30:70), (b) 165 nm (70:30), and (c) 470 nm (70:30). First order reflection peaks are represented by circles.

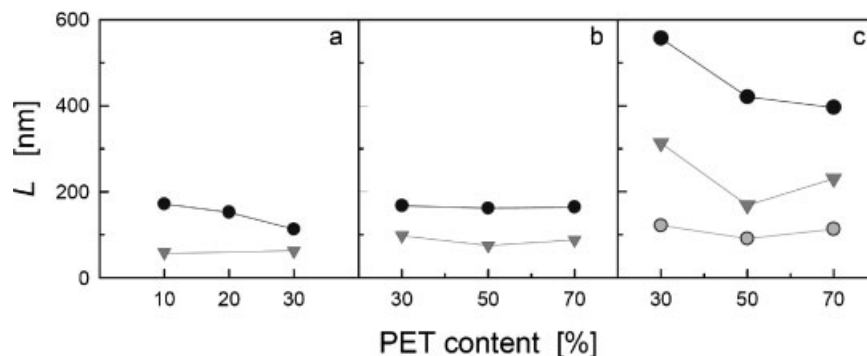


Figure 7. USAXS spacings, as a function of PET content, for PET/PC samples with nominal repeating distance L_{nom} of: (a) 85 nm (10:90, 20:80, and 30:70); (b) 165 nm (30:70, 50:50, and 70:30); and (c) 470 nm (30:70, 50:50, and 70:30). First order peaks are represented by circles.

Influence of PET Content

Let us next consider what is the effect of changing the volume ratio of the material, i.e., the proportion of PET in relation to PC, in the corresponding nanostructure. Again, to increase the contrast, all the samples were annealed at the same temperature, $T_a = 150^\circ\text{C}$, for 30 min. Figure 7 shows the USAXS spacings for the three investigated nominal interlayer distances L_{nom} as a function of material composition. It is found that, with decreasing PET content and after normalizing to film thickness, the long spacings tend to increase. Such behavior could be explained, as mentioned before, by the breakup of the thinnest layers.

Finally, if one plots the peak area (scattering intensity) of the same set of materials of Figure 7, as a function of the volume ratio of PET, the opposite behavior is detected (Figure 8); i.e., the scattering intensity rises with increasing PET content. This tendency still remains after correcting for the effect related to the volume fraction variation $v(1-v)$ [second term in Equation (1)]. Specifically, in the case of the samples with PET/PC volume ratios of 30:70 and 70:30 and

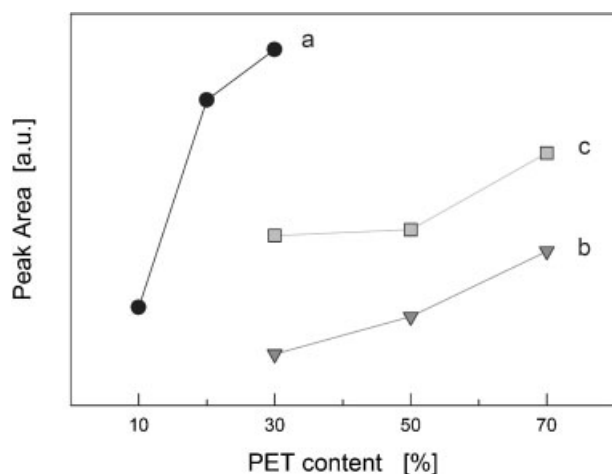


Figure 8. Variation of total peak area (scattering intensity) with increasing PET content. Data points in lines a, b, and c correspond to samples a, b, and c in Figure 7, respectively.

according to the Babinet's reciprocity theorem, they should yield identical scattered intensities. However, the observed USAXS intensity is always higher for the 70:30 nanolayers.

It means that the layer thickness distribution for the material with higher PET content should be narrower than for the other case. These observations lead to the conclusion that the PET/PC systems where the presence of PET is larger, develop a more regular layered structure.

Conclusion

The use of USAXS, with the X-ray beam slightly rotated from a parallel configuration with respect to the PET/PC nanolayered film surfaces, reveals the occurrence of scattering maxima corresponding to the stacking periodicities. Annealing of the nanolayered films mainly provokes the crystallization of PET; consequently the scattering maxima are more clearly developed due to the increase in the electron density difference between the alternating polymer layers.

The experimental long spacings for semicrystalline/amorphous nanolayers, derived from USAXS, show values which correlate fairly well with the nominal periodicity values of the stacks prepared by the co-extrusion method. AFM images of some of the materials reveal periodicities which are also in good agreement with the USAXS data.

It has been observed that increasing the volume ratio of PET in the PET/PC system seems to favor the development of the nanolayered structure.

The appearance of at least two scattering peaks in all investigated cases, corresponding to higher orders of the same repeating distance, accounts for the high regularity of the nanostructure that can be obtained by means of the co-extrusion processing technique.

Acknowledgements: The generous support from the MEC, Spain (grant FIS2004-01331) is gratefully acknowledged. This research was also supported by the NSF Center for Layered Polymeric

Systems (grant DMR-0349436) and the European Community – Research Infrastructure Action under the FP6 “Structuring the European Research Area” Program (through the Integrated Infrastructure Initiative “Integrating Activity on Synchrotron and Free Electron Laser Science.”) Contract RII3-CT-2004-506008.

Received: December 20, 2007; Revised: April 2, 2008; Accepted: April 9, 2008; DOI: 10.1002/macp.200700639

Keywords: atomic force microscopy (AFM); co-extrusion; nanolayers; structure; ultra-small-angle X-ray scattering (USAXS)

- [1] B. Jérôme, J. Commandeur, *Nature* **1997**, *386*, 589.
- [2] J. A. Forrest, K. Dalnoki-Veress, J. R. Dutcher, *Phys. Rev. E* **1997**, *56*, 5705.
- [3] O. Prucker, S. Christian, H. Bock, J. Rühle, C. W. Frank, W. Knoll, *Macromol. Chem. Phys.* **1998**, *199*, 1435.
- [4] J. Mattsson, J. A. Forrest, L. Börjesson, *Phys. Rev. E* **2000**, *62*, 5187.
- [5] J. A. Forrest, K. Dalnoki-Veress, *Adv. Colloid Interface Sci.* **2001**, *94*, 167.
- [6] F. J. Balta Calleja, F. Ania, I. Puente Orench, E. Baer, A. Hiltner, T. E. Bernal-Lara, S. Funari, *Prog. Colloid Polym. Sci.* **2005**, *130*, 140.
- [7] R. Y. F. Liu, Y. Jin, A. Hiltner, E. Baer, *Macromol. Rapid Commun.* **2003**, *24*, 943.
- [8] R. Y. F. Liu, T. E. Bernal-Lara, A. Hiltner, E. Baer, *Macromolecules* **2004**, *37*, 6972.
- [9] P. Müller-Buschbaum, *Anal. Bioanal. Chem.* **2003**, *376*, 3.
- [10] H. Matsuoka, Y. Nakatani, M. Yamakawa, N. Ise, *J. Phys.* **1993**, *IV 3 (C8)*, 451.
- [11] N. Hermsdorf, M. Stamm, S. Forster, S. Cunis, S. S. Funari, R. Gehrke, P. Müller-Buschbaum, *Langmuir* **2005**, *21*, 11987.
- [12] C. G. Zhao, G. J. Hu, R. Justice, D. W. Schaefer, S. M. Zhang, M. S. Yang, C. C. Han, *Polymer* **2005**, *46*, 5125.
- [13] D. R. Rueda, F. Ania, F. J. Baltá Calleja, *Polymer* **1997**, *38*, 2027.
- [14] T. Koga, T. Koga, T. Hashimoto, *J. Chem. Phys.* **1999**, *110*, 11076.
- [15] E. M. Ivan'kova, G. H. Michler, A. Hiltner, E. Baer, *Macromol. Mater. Eng.* **2004**, *289*, 787.
- [16] R. Adhikari, W. Lebek, R. Godehardt, S. Henning, G. H. Michler, A. Hiltner, E. Baer, *Polym. Adv. Technol.* **2005**, *16*, 95.
- [17] I. Puente-Orench, F. Ania, E. Baer, A. Hiltner, T. Bernal, F. J. Baltá-Calleja, *Philos. Mag.* **2004**, *84*, 1841.
- [18] R. Y. F. Liu, T. E. Bernal-Lara, A. Hiltner, E. Baer, *Macromolecules* **2005**, *38*, 4819.
- [19] S. V. Roth, R. Dörhmann, M. Dommach, M. Kuhlmann, I. Kröger, R. Gehrke, H. Walter, C. Schroer, B. Lengeler, P. Müller-Buschbaum, *Rev. Sci. Instr.* **2006**, *77*, 085106.
- [20] F. Ania, F. J. Balta Calleja, I. Puente Orench, S. Roth, E. Baer, A. Hiltner, T. E. Bernal-Lara, *HASYLAB Annual Report*, 2005, 887. http://hasylab.desy.de/science/annual_reports/hasylab_annual_reports/2005/index_eng.
- [21] J. Wu, *Polymer* **2003**, *44*, 8033.
- [22] N. Stribeck, “X-ray Scattering of Soft Matter”, Springer-Verlag, Berlin 2007.
- [23] T. E. Bernal-Lara, R. Y. F. Liu, A. Hiltner, E. Baer, *Polymer* **2005**, *46*, 3043.